



Column leaching of low-grade saprolitic laterites and valorization of leaching residues

Kostas Komnitsas^{a,*}, Evangelos Petrakis^a, Georgios Bartzas^b, Vassiliki Karmali^a

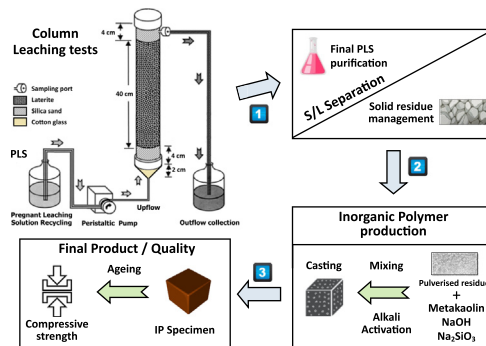
^a Technical University of Crete, School of Mineral Resources Engineering, University Campus, Kounoupidiana, 73100 Chania, Greece

^b National Technical University of Athens, School of Mining and Metallurgical Engineering, 9 Heron Polytechniou str., 157 80 Zografos, Athens, Greece

HIGHLIGHTS

- Low grade saprolitic laterites are column leached for the extraction of Ni and Co.
- The presence of Na₂SO₃ has a beneficial effect on Ni and Co extraction.
- The selectivity of leaching is good considering the ratio Ni/Fe in the PLS.
- Leaching residues can be successfully alkali activated.
- The inorganic polymers produced have low toxicity and high compressive strength.

GRAPHICAL ABSTRACT



ARTICLE INFO

Article history:

Received 17 December 2018

Received in revised form 28 January 2019

Accepted 28 January 2019

Available online 30 January 2019

Editor: Damia Barcelo

Keywords:

Saprolitic laterites
Column leaching
Sulfuric acid
Sodium sulfite
Inorganic polymers

ABSTRACT

Socio-economic data on nickel and cobalt show their importance throughout the entire metal value chain, from mining to end use, disposal and recycling. Thus, the extraction of both metals from primary and secondary raw materials as well as from wastes is currently considered strategically important for the industry and the society. In this paper heap leaching of Greek low-grade saprolitic laterites, with Ni content 0.97%, was investigated. The main parameters studied involved the strength of the H₂SO₄ solution used (49 and 147 g L⁻¹) and the effect of adding sodium sulfite (Na₂SO₃) in the leaching medium. The pregnant leach solution (PLS) was recycled several times during leaching in order to minimize acid consumption. The experimental results showed that within a period of 25 days, and under the optimum conditions (147 g L⁻¹ H₂SO₄ and 20 g L⁻¹ Na₂SO₃), i) Ni and Co extractions were 72.5% and 47.4%, respectively and ii) Fe and Al co-extractions were 8.7% and 31.3%, respectively. Furthermore, valorization of the leaching residues through alkali activation using NaOH and Na₂SiO₃ and the addition of metakaolin (MK) for the production of inorganic polymers (IPs) was explored. X-ray fluorescence (XRF), X-ray diffraction (XRD), Fourier-transform infrared (FTIR) spectroscopy, Differential scanning calorimetry (DSC/TG) and Scanning electron microscopy (SEM-EDS) were used to characterize the ore, its leaching residues and the IPs. The IPs produced demonstrated high compressive strength, almost 40 MPa and are suitable for a wide range of applications in the construction sector.

© 2019 Elsevier B.V. All rights reserved.

1. Introduction

Nickel and cobalt have excellent physical and chemical properties and thus they are essential for thousands of products. Both metals are

* Corresponding author.

E-mail address: komni@mred.tuc.gr (K. Komnitsas).

also necessary for the most common types of lithium-ion batteries which power electric vehicles. The annual production and consumption of nickel exceeds two million tonnes. On the other hand, the annual European Union (EU) cobalt production is almost 2300 t, while its demand is about nine times higher and is met by imports from third countries (EU Science Hub, 2019; Nickel Institute, 2019).

Nickel laterites are formed through weathering of underlying parent rocks and the resulting main zones of mineralization include limonites (with high iron and low magnesium content) and saprolites (with high magnesium and low iron content). Saprolites, which are more reactive compared to limonites, are located at the bottom of the deposit and contain nickel-rich serpentines and hydrous magnesium silicates (Luo et al., 2009; Myagkiy et al., 2017). Due to the complexity of the laterite ores and the presence of nickel in several mineral phases, their beneficiation with the use of traditional mineral processing techniques, including gravity-, electrostatic-, magnetic-, and density separation, as well as flotation, is quite inefficient. Selective grinding aiming at separation of the coarse fraction, which normally has a lower Ni content, is rarely successful (Petrakis et al., 2018; Quast et al., 2015).

The continuous depletion of higher grade nickel sulfides and the increasing demand for nickel, which is used in many industrial products including Li-ion battery cathodes in electric vehicles, requires the economical treatment of the huge reserves of nickel laterites (MacCarthy et al., 2015).

Today, most nickel laterites, which represent almost 70% of the global reserves, are low grade (<1.5%) and account for almost 40% of nickel production. These ores are mainly treated pyrometallurgically to produce ferronickel (FeNi) (Pickles and Anthony, 2018). However, due to the high environmental footprint of pyrometallurgical treatment (Bartzas and Komnitsas, 2015; Eckelman, 2010), research efforts are focusing on the development of more economical and eco-friendly hydrometallurgical approaches (Khoo et al., 2017; Norgate and Jahanshahi, 2011; Quast et al., 2013).

The main hydrometallurgical techniques include atmospheric leaching (McDonald and Whittington, 2008), heap leaching (Oxley et al., 2016), high pressure acid leaching (HPAL) (Loveday, 2008; Zhang et al., 2015) and bioleaching (du Plessis et al., 2011; Le et al., 2006). Other alternatives including pre-roasting and acid leaching have been also investigated (Li et al., 2018a, 2018b; Li et al., 2009).

Atmospheric leaching is carried out at ambient temperature in stirred reactors and is often characterized by low selectivity. It involves the use of sulfuric (Luo et al., 2010; Thubakgale et al., 2013), hydrochloric (Guo et al., 2015; Mystrioti et al., 2018) or ammonium chloride-hydrochloric acid mixtures (Li et al., 2018a, 2018b). Bioleaching still requires process optimization in order to improve its efficiency and economics (Chaerun et al., 2017; Jang and Marjorie Valix, 2017).

HPAL, which is carried out with the use of sulfuric acid, nitric acid or ferric chloride, is characterized by high recoveries of Ni and Co, low recoveries of Fe and Al, short leaching times but high operating costs (Liu et al., 2012; Ma et al., 2015; Zhang et al., 2016). An excellent continuous model for sulfuric acid pressure leaching of laterites has been proposed by Rubisov and Papangelakis (2000).

Heap leaching, which is considered a feasible alternative for the treatment of low grade laterite ores, has been intensively investigated over the last years. It is characterized by slower kinetics, longer leaching times, which normally vary between 60 and 100 days, and higher selectivity compared to leaching in stirred reactors (Elliot et al., 2009; Quaicoe et al., 2014; Quast et al., 2013; Watling et al., 2011).

Laterites are treated for >50 years at the pyrometallurgical plant of Larymna, in central Greece, to produce FeNi (Zevgolis et al., 2010). The atmospheric and pressure leaching of Greek laterites was first studied in the '80s (Komnitsas, 1983; Komnitsas, 1988; Kontopoulos and Komnitsas, 1988; Panagiotopoulos et al., 1986). Later, heap leaching was intensively investigated in laboratory and pilot tests (Agatzini-Leonardou and Dimaki, 1994; Agatzini-Leonardou and Zafiratos, 2004; Agatzini-Leonardou et al., 2004; Agatzini-Leonardou et al., 2009).

Recently, by taking into account the gradual depletion of the ore grade and the increased demand for nickel, research efforts have been again initiated (Komnitsas et al., 2018; Mystrioti et al., 2018).

In this context, the main aim of this study was to investigate the efficiency of column leaching with the use of sulfuric acid (H₂SO₄) for the treatment of low-grade Greek saprolitic laterites as well as to study the effect of the addition of sodium sulfite (Na₂SO₃) in the leaching solution on the overall efficiency of the process. The study also aimed to explore the potential of alkali activation for the valorization of leaching residues in order to improve process economics and reduce environmental impacts associated with their disposal.

2. Materials and methods

2.1. Ore

The ore used in this study is a saprolitic laterite (<30 mm, 0.97%wt Ni) which was obtained from Larco S.A mines in Kastoria (Northern Greece). The ore (100 kg) was homogenized by the cone and quartering method and a representative sample of about 1 kg was crushed below 4 mm for the determination of the particle size distribution.

2.2. Leaching tests

Three leaching tests were carried out in laboratory Plexiglas columns, with 5 cm inner diameter and 50 cm height, to study the effect of (i) H₂SO₄ concentration and (ii) the addition of Na₂SO₃ in the leaching solution on Ni, Co and other elements extraction. The column experimental conditions are presented in Table 1. 1000 g of laterite ore (LK) were added in the main column zone so that a bed of 40 cm height was formed. Two 4 cm layers of silica sand were placed at both ends of each column to act as filters. Cotton glass was also added at the bottom of each column to prevent losses of ultra-fine particles and avoid clogging of the columns. The experimental configuration is shown in Fig. 1.

It is important to note that the experimental conditions used were carefully selected based on the results of earlier tests investigating leaching of other Greek saprolitic and limonitic ores (Komnitsas et al., 2018).

Upflow transport of the leaching medium with the use of peristaltic pumps (Masterflex L/S economy variable-speed drive, Cole-Parmer Instrument Co) was considered to enable full contact of the leaching medium with the ore. The leaching solution was pumped from 5 L plastic vessels with a flow-rate of 3 L day⁻¹ and collected in the outflow in similar vessels. The duration of each leaching test, which involved daily recycling of the PLS, was 25 days, while at the end of the tests, columns were flushed with distilled water so that the final PLS volume was ~3 L. 10 mL samples from the outflow were initially collected daily and at later stages every 2 or 3 days to measure pH and Eh with the use of a WTW pH 7110 inoLab pH/Eh meter and determine the concentration of Ni, Co, Fe, Ca, Al, Mg and Mn in the PLS by atomic absorption spectroscopy (AAS). Acid consumption was calculated using the titrimetric method proposed by Quaicoe et al. (2014). The efficiency of leaching was determined by taking into account the extraction percentage of the useful elements Ni and Co as well as by calculating the ratios Ni/Fe, Ni/Mg, Ni/Ca and Ni/Al in the PLS, given that Fe, Mg, Ca and Al are the undesirable elements. All leaching tests were carried out in duplicate and mean values are given for all parameters analysed; it is

Table 1
Column experimental conditions.

| Test no. | H ₂ SO ₄ solution (g L ⁻¹) | Na ₂ SO ₃ concentration (g L ⁻¹) |
|----------|--|--|
| 1 | 49 | - |
| 2 | 147 | - |
| 3 | 147 | 20 |

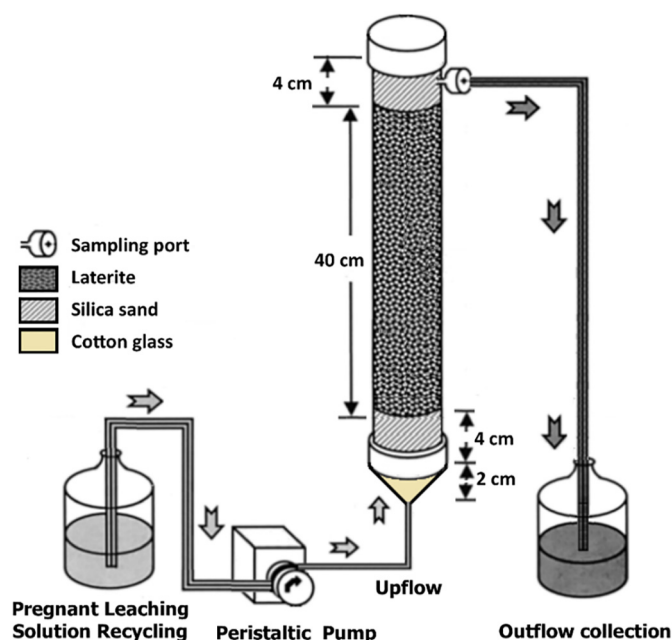


Fig. 1. Experimental configuration of column leaching tests.

mentioned though that the variation of measurements was in all cases around $\pm 1\%$.

2.3. Valorization of leaching residues

The valorization of the leaching residues (LKr) was investigated through alkali activation. The residues were first dried at $80\text{ }^{\circ}\text{C}$ for 1 day, then pulverized using a FRITSCH BICO pulverizer ($d_{90} = 52.4\text{ }\mu\text{m}$) and added under continuous slow mixing to the activating solution, consisting of NaOH and sodium silicate ($\text{Na}_2\text{O} = 7.5\text{--}8.5\%$, $\text{SiO}_2 = 25.5\text{--}28.5\%$, Merck). The NaOH solution was prepared by dissolving sodium hydroxide anhydrous pellets (Sigma Aldrich) in distilled water, until the required molarity was obtained. The effect of the addition of metakaolin in the starting mixture (5 and 10%wt) as filler, for the supply of Al^{3+} ions in the inorganic polymer paste, as well as the calcination of the LKr at 800 and $1000\text{ }^{\circ}\text{C}$ in order to increase its reactivity were also examined. Metakaolin was produced after calcining kaolin, $\text{Al}_2\text{Si}_2\text{O}_5(\text{OH})_4$ (Fluka) at $750\text{ }^{\circ}\text{C}$ for 2 h in a SNOL 8,2/1100 oven. Calcination of LKr was carried out for 1 h in the same oven. Loss on ignition (LOI) was determined by heating the materials at $1050\text{ }^{\circ}\text{C}$ for 4 h.

The liquid to solid (L/S) ratio was adjusted in order to improve the flowability of the paste before casting. A typical indicative composition of the mixture included (in %wt): leaching residue 69%, metakaolin 7%, 8 M NaOH solution 12% and Na_2SiO_3 12%. The fresh paste was cast in cubic metal moulds of 5 cm edge, which were vibrated for a few minutes to eliminate the presence of air voids in the reactive mass. The moulds remained at room temperature for 2 h to allow early initiation of the alkali activating reactions, development of structural bonds and early solidification of the paste. Then the specimens were demoulded, sealed in plastic bags to prevent fast evaporation of water, cured at $80\text{ }^{\circ}\text{C}$ in a laboratory oven (Jeio Tech ON-02G) for 24 h and then allowed to cool. This configuration was based on the results obtained from previous studies investigating the alkali activation potential of several metallurgical wastes (Komnitsas et al., 2007; Zaharaki et al., 2016). After ageing at room temperature for 7 days, the compressive strength of the specimens was determined with the use of a MATEST C123N load frame. All tests were carried out in triplicate.

Finally, the toxicity of the leaching residues as well as of the specimens produced after alkali activation was assessed by using the EN 12457-3 test (EN12457-3:2002; van der Sloot et al., 2001), which

involves leaching of material in distilled water (8 L kg^{-1}) for 24 h. The obtained solutions were filtered using $0.45\text{ }\mu\text{m}$ membrane filters and the concentration of the metals in the eluate was expressed as mg kg^{-1} of dry sample and compared with existing limits for disposal of wastes in different landfills (European Commission, 2002). Apart from distilled water a more severe leaching agent, namely an HCl solution with pH 4, was used.

2.4. Use of analytical techniques

After grinding with the use of a FRITSCH-BICO pulverizer, the ore (LK) and the leaching residues (LKr) were chemically and mineralogically characterized using (i) a Bruker-AXS S2 Range type X-ray fluorescence energy dispersive spectrometer (XRF-EDS) and (ii) an X-ray diffractometer (XRD), D8 ADVANCE type (BRUKER-AXS). Chemical analysis of the ore and each leaching residue was also carried out after digestion of 2 g of each sample in aqua regia followed by AAS, with a Perkin Elmer AAnalyst 100 Flame Atomic Absorption Spectrometer. Since the differences observed between XRF and AAS results were minor ($\pm 1\%$), those obtained by XRF are presented in this study. The functional groups in each solid sample were identified by Fourier transform infrared (FTIR) spectroscopy, using a Perkin Elmer Spectrum 1000 spectrometer, while a Setaram LabSys Evo analyzer was used for Differential Scanning Calorimetry and Thermogravimetry (DSC/TG).

Scanning electron microscopy (SEM) and energy dispersive X-ray spectroscopy (EDS) were used to evaluate the morphology of the ore and the solid leaching residues. A JEOL-6380LV scanning microscope (Tokyo, Japan) operating at an accelerating voltage of 20 kV was used. Back-scattered electron (BSE) examinations were carried out on polished sections of the samples embedded in epoxy resin to ensure cohesion of the solid residues.

3. Results and discussion

3.1. Characterization of the ore

The cumulative particle size distribution of the $\sim 4\text{ mm}$ LK ore is presented in Fig. 2. The results show that the 80% passing size (d_{80}) is 2.1 mm. The chemical composition (Table 2) confirms that the ore is a saprolitic low grade laterite, with high magnesia and low iron content.

3.2. Leaching efficiency

Fig. 3(a–g) show the percent extraction of Ni, Co, Fe, Mg, Al, Mn and Ca as a function of time. As shown in Fig. (3a) Ni extraction obtained after 25 days of leaching with the use of 49 g L^{-1} H_2SO_4 solution (0.5 M) is low and does not exceed 14% whereas, the increase of acid

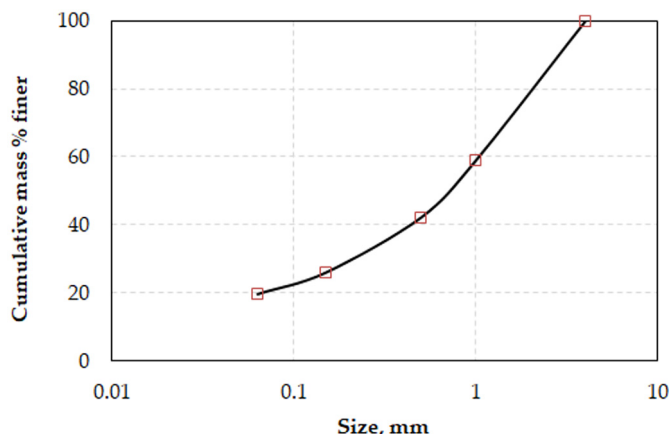


Fig. 2. Particle size distribution of Kastoria laterite (LK) ore.

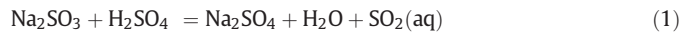
Table 2
Chemical composition (%wt) of LK ore.

| Ni | Co | Fe ₂ O ₃ | SiO ₂ | Al ₂ O ₃ | MgO | MnO | CaO | Cr ₂ O ₃ | LOI ^a |
|------|-------|--------------------------------|------------------|--------------------------------|-------|------|------|--------------------------------|------------------|
| 0.97 | 0.031 | 21.79 | 34.44 | 0.35 | 17.14 | 0.33 | 7.16 | 0.86 | 16.8 |

^a LOI: loss on ignition.

strength to 147 g L⁻¹ H₂SO₄ (1.5 M) improves Ni extraction to 47%. Cobalt extraction follows a similar trend (Fig. 3b) and increases from 11.3% to 27.9% with the increase in acid strength. Higher extractions of 72.5% and 47.4% for Ni and Co respectively, were obtained when Na₂SO₃ was added to the leaching solution. It is noteworthy that the increase of Ni

and Co extractions in the presence of Na₂SO₃ was very fast within 2–4 days (Komnitsas et al., 2018; Luo et al., 2015). In the presence of higher concentrations of Na₂SO₃ (30 g L⁻¹), the increase of Ni and Co extractions was only marginal (~1%, data not shown). In the presence of H₂SO₄, Na₂SO₃ reacts with H⁺ ions to form the intermediate H₂SO₃ which dissociates to SO₂ (Reaction (1):



The SO₂(aq) from Reaction (1) reacts with iron-based phases (e.g. goethite), as shown in Reaction (2), accelerates Fe extraction and subsequently Ni release from the iron phases (Das and de Lange, 2011). The generation of SO₂ is clearly visible in the first days of leaching through

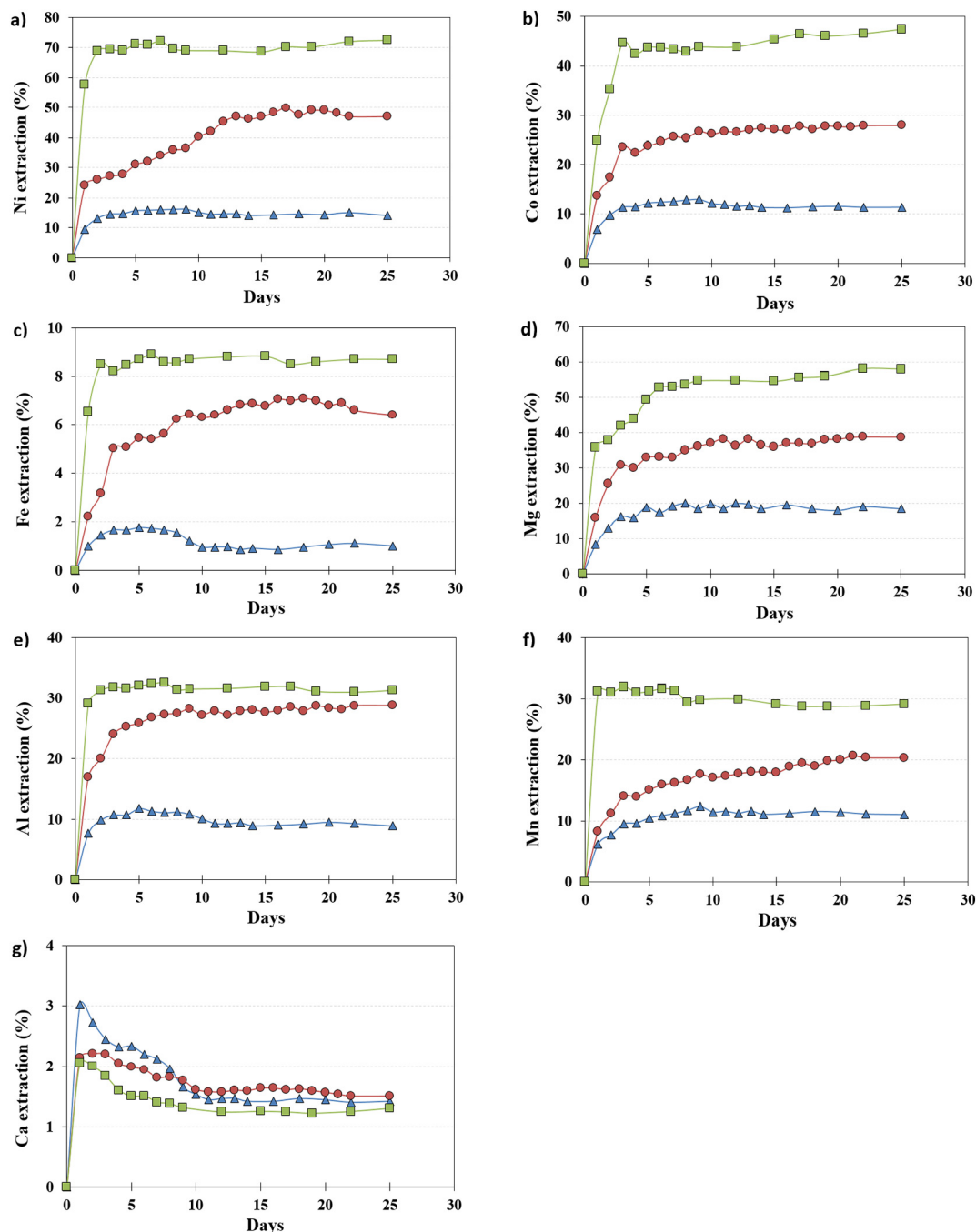
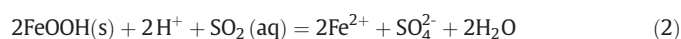


Fig. 3. Evolution of % metal extraction vs. time during LK leaching, ▲: 49 g L⁻¹ H₂SO₄, ●: 147 g L⁻¹ H₂SO₄, ■: 147 g L⁻¹ H₂SO₄ containing 20 g L⁻¹ Na₂SO₃.

Table 3
PLS composition and selectivity of leaching.

| Test no. | mg L ⁻¹ | | | | | | Ni/Fe | Ni/Mg | Ni/Ca | Ni/Al |
|----------|--------------------|------|------|--------|-----|-----|-------|-------|-------|-------|
| | Ni | Co | Fe | Mg | Ca | Al | | | | |
| 1 | 501 | 12.9 | 563 | 7005 | 267 | 61 | 0.89 | 0.07 | 1.88 | 8.21 |
| 2 | 1600 | 30.3 | 3423 | 14,002 | 269 | 186 | 0.47 | 0.11 | 5.95 | 8.60 |
| 3 | 2825 | 59.3 | 5328 | 24,001 | 260 | 233 | 0.53 | 0.12 | 10.87 | 12.12 |

the production of bubbles within the column bed. It is mentioned that in other tests carried out in our laboratory using higher solution flowrates, a synergistic effect of flowrate and bubbles was noted and the ore bed was split in several parts and lifted



Reaction (2) requires less acid for the dissolution of goethite than Reaction (3) which involves direct leaching of iron-based phases (Georgiou and Papangelakis, 1998)



Fig. 3(c) shows that the extraction of Fe increases in all tests with the increase of acid strength or the addition of Na₂SO₃ but it remains in general very low (<9%) and thus the selectivity of leaching is improved. The low Fe extraction obtained in these column tests is due to the milder conditions used, namely low temperature and coarser feed size, compared to stirred reactor leaching (Mystrioti et al., 2018).

The maximum co-extraction of other elements, namely Mg, Al, Mn and Ca, which also assesses the selectivity of leaching, was 58%, 31.3%, 29.1% and 1.3%, respectively, as seen in Fig. 3(d–g).

The similar profiles of Ni and Mg extraction indicate that Ni is loosely bound in Ni-containing phases such as lizardite and thus both elements can be leached simultaneously (Luo et al., 2010). On the other hand, the extraction of Ni which is associated to magnetite/maghemite and chromite is difficult since these phases remain practically unleached (Canterford, 1986).

The pH of the leaching solutions was very low in all tests, increased slowly with time but did not exceed the value of 1.5. When the leaching solution contained 147 g L⁻¹ H₂SO₄ and 20 g L⁻¹ Na₂SO₃, Eh values decreased gradually with time from 385 to 282 mV (Komnitsas et al., 2018). The beneficial effect of the reducing agent Na₂SO₃ in lowering the potential of the leaching reactions and increasing the extraction of nickel contained in the iron phases has been also noticed during atmospheric sulfuric acid leaching of limonitic laterites at temperatures between 30 and 90 °C (Luo et al., 2015). The weight loss recorded during leaching was quite similar in all tests and varied between 16.1% (when a solution with 49 g L⁻¹ H₂SO₄ was used) and 18.8% (when a solution containing 147 g L⁻¹ H₂SO₄ and 20 g L⁻¹ Na₂SO₃ was used).

Table 4
Results of various column leaching studies for saprolitic ores.

| Ni content (%) | Particle size (mm) | H ₂ SO ₄ (g L ⁻¹) | Duration (days) | Flow rate (L day ⁻¹) | Extraction (%) | | | Ni/Fe in PLS | Acid consumption (kg t ⁻¹ ore) | Reference |
|----------------|--------------------|---|-----------------|----------------------------------|----------------|------|------|--------------|---|--|
| | | | | | Ni | Fe | Co | | | |
| 1.94 | <15 ^a | 98 | 10 | 4.0 | 60.0 | 12.6 | 45.0 | 0.7–1.0 | 510 | Agatzini-Leonardou and Zafiratos, 2004 |
| 1.20 | <20 | 100 | 122 | 31.4 | 83.9 | 55.8 | 55.2 | 0.11 | 462 | Büyükkakinci, 2008 |
| 0.92 | <15 ^a | 200 | 101 | 2.3 | 97.0 | – | 75.0 | – | 502 | Nosrati et al., 2014 |
| 0.92 | <2 ^a | 200 | 100 | 2.3 | 90.0 | 60.0 | 72.8 | 0.06 | 641 | Quaicoe et al., 2014 |
| 0.97 | <4 | 147 | 25 | 2.5 | 47.0 | 6.4 | 27.9 | 0.47 | 626.2 | This study |
| 0.97 | <4 | 147 ^b | 25 | 2.5 | 72.5 | 8.7 | 47.4 | 0.53 | 576.8 | |

^a Agglomerated feed ore.

^b + Addition of sodium sulfite.

Table 5
Comparative results obtained after leaching of a Greek limonitic and saprolitic laterite ore.

| Ore type ^a | Ni (%) | H ₂ SO ₄ (g L ⁻¹) | Duration (days) | Extraction (%) | | | Ni/Fe in PLS | Reference |
|-----------------------|--------|---|-----------------|----------------|-----|------|--------------|------------------------|
| | | | | Ni | Fe | Co | | |
| L | 0.58 | 147 | 33 | 60.2 | 3.9 | 59.0 | 0.26 | Komnitsas et al., 2018 |
| L | 0.58 | 147 ^b | 33 | 73.5 | 7.9 | 84.1 | 0.15 | This study |
| S | 0.97 | 147 | 25 | 47.0 | 6.4 | 27.9 | 0.47 | |
| S | 0.97 | 147 ^b | 25 | 72.5 | 8.7 | 47.4 | 0.53 | |

^a L: limonitic ore, S: saprolitic ore.

^b Addition of sodium sulfite.

The concentrations of the main elements (mg L⁻¹) in the PLS are presented in Table 3. This table also compares the selectivity of leaching as defined by the concentration ratios of Ni/Fe, Ni/Mg, Ni/Ca, and Ni/Al. Because low Ni and Co extractions are obtained when 49 g L⁻¹ H₂SO₄ solution is used as leaching medium, the comparison does not include the results of this test. The results indicate that the addition of Na₂SO₃ in the leaching medium, apart from the fast extraction of Ni, improves also the selectivity of leaching since the ratios Ni/Fe, Ni/Mg, Ni/Ca, and Ni/Al increase by 13%, 9%, 83% and 41%, respectively.

Table 4 presents comparative results of various studies involving column leaching of saprolitic ores, as derived from the related literature. It is seen that the efficiency of leaching depends on Ni grade, ore size, agglomeration of feed, concentration of acid, flowrate of leaching solution and duration of column tests. Apart from these factors, the type of laterite is also crucial during leaching (MacCarthy et al., 2016; McDonald and Whittington, 2008). Table 5 presents the results of the this and a recent similar study that involved column leaching of a Greek limonitic ore (L), with a much lower Ni grade (Komnitsas et al., 2018). These data show that despite the higher extraction of Ni and the lower extraction of Fe from the limonitic ore, a much lower (45–72%) Ni/Fe ratio was recorded in the PLS due to its much lower Ni grade. Also, much higher Co extractions were obtained during leaching of the limonitic ore in all cases studied. The results of earlier laterite column leaching studies showed that for limonitic ores, dissolution of the refractory iron minerals, such as goethite, is required to obtain high Ni and Co extractions, whereas for saprolitic ores the Ni and Co bearing silicate minerals are weakly bound and hence the extraction of both elements contained in them is much easier (Quaicoe et al., 2014; Watling et al., 2011). However, as indicated in an excellent recent study, given the intrinsic mineral heterogeneity of Ni-laterites, a comprehensive mineralogical characterization at the mineral grain scale is required in order to assess the overall leaching behavior of the ore. In the same study it is mentioned that the scale of leaching tests may also affect Ni and Fe selectivity (Hunter et al., 2013).

3.3. Alkali-activation of residues

After heap leaching, the residues are normally transferred to a lined facility, which is called spent ore repository and are reclaimed with the

Table 6

Typical composition of LKr obtained after leaching of laterite ore with $147 \text{ g L}^{-1} \text{ H}_2\text{SO}_4$ and $20 \text{ g L}^{-1} \text{ Na}_2\text{SO}_3$.

| Fe ₂ O ₃ | SiO ₂ | Al ₂ O ₃ | MgO | MnO | CaO | Cr ₂ O ₃ | TiO ₂ | LOI ^a | Total |
|--------------------------------|------------------|--------------------------------|------|------|------|--------------------------------|------------------|------------------|-------|
| 16.43 | 39.71 | 0.54 | 4.45 | 0.11 | 7.96 | 2.35 | 0.84 | 27.11 | 99.5 |

^a LOI: loss on ignition.

construction of a vegetative soil cover (Zanbak, 2012). Thus, valorization of the residues and production of added value materials will reduce the overall cost of the process and minimize its environmental impacts.

The chemical analysis of the residues obtained after LK leaching is presented in Table 6. It is seen that while the residues contain sufficient SiO₂, the content of Al₂O₃ remains low.

It is known that alkali activation of Al-Si wastes and residues in relatively low temperature (40–90 °C) results in the formation of dense IPs with chemical composition similar to zeolites and amorphous to semi-crystalline three-dimensional aluminosilicate microstructure. The produced materials are mainly called IPs (also known as geopolymers) (Komnitsas and Zaharaki, 2007). Fig. 4 shows the compressive strength of the IPs produced after alkali activation of the residues (LKr) obtained after LK leaching. The effect of the addition of 5 and 10%wt metakaolin as well as the calcination of the residues at 800 and 1000 °C is also presented. These results indicate that (i) the residues obtained after laterite leaching cannot be alkali activated and the compressive strength of the produced specimens merely reaches 1.3 MPa, (ii) mixing with 10%wt metakaolin results in a noticeable increase of the compressive strength of the specimens, to 39 MPa, (iii) calcination of LKr at 800 °C (LKr800) and 1000 °C (LKr1000) has adverse effect on the compressive strength.

LKr have low content of Al (Table 6) and therefore cannot be alkali activated. There is no specific rule about the ratio SiO₂:Al₂O₃ in the starting mixture but this has to be quite high provided that the content of both oxides is sufficient. For example, ferronickel slag produced after pyrometallurgical treatment of the same laterites is well alkali activated since the aforementioned ratio is ~4 (SiO₂ 32.74%, Al₂O₃ 8.32%) (Komnitsas and Zaharaki, 2007). Thus, in order to increase the alkali activation potential of LKr (SiO₂:Al₂O₃ = 73.5, Al₂O₃ content only 0.54%) an Al source is required. The results show that the addition of 5% and especially 10%wt MK, with an Al₂O₃ content of ~30% (Kwon et al., 2017;

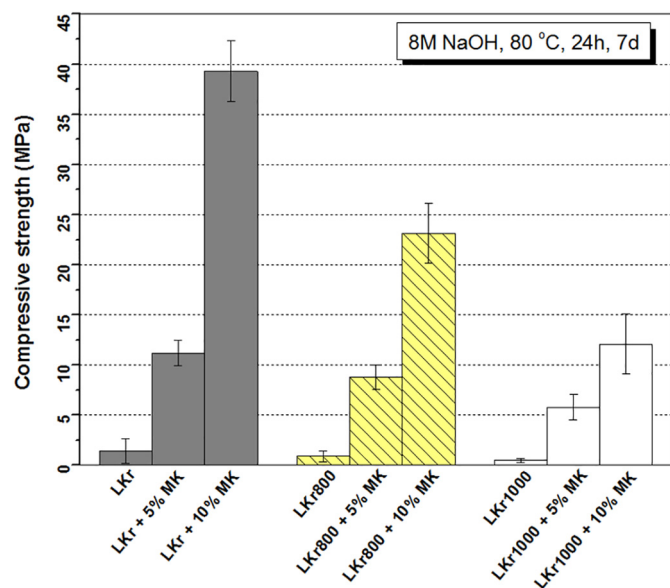


Fig. 4. Effect of the addition of metakaolin (MK) (5 and 10%wt) and calcination on the compressive strength of specimens produced by alkali activation of LKr. Conditions were: 8 M NaOH, heating at 80 °C for 24 h, curing for 7 days. LKr: Kastoria laterite leaching residue, LKr800: leaching residue calcined at 800 °C, LKr1000: leaching residue calcined at 1000 °C.

Sullivan et al., 2018), improves greatly their alkali activation potential, because calcination of kaolin changes its original crystalline structure. The dehydration starts at about 100–120 °C, then dehydroxylation of the structure takes place and finally metakaolin is produced. The loss of crystallinity weakens the bonds between crystals and the produced metakaolin has sufficient amorphous content and thus exhibits increased reactivity during alkali activation. It is also known that calcination of kaolin transforms the octahedral coordinated Al layers into the more reactive tetrahedral form. It is thus anticipated that Al ions may dissolve more rapidly from metakaolin than from un-calcined kaolin (Komnitsas et al., 2009). The percentage of Na₂SiO₃ used in the present study was carefully selected after a number of tests in order to balance the SiO₂:Al₂O₃ ratio.

3.4. Characterization of the leaching residues

Fig. 5 presents the XRD patterns of LK ore and selected LKr. The main mineralogical phases present in the ore are: quartz (SiO₂), goethite (FeO (OH)) and magnesium-bearing silicates, such as lizardite [(Mg,Fe)₃Si₂O₅(OH)₄], (clino)chrysotile [Mg₃Si₂O₅(OH)₄] and saponite [Ca_{0.5}(Mg,Fe)₃(Si,Al)₄O₁₀(O,H)₂·4H₂O], while the main Ni-bearing phases are nepouite [(Ni,Mg)₃Si₂O₅(OH)₄] and chromite (FeCr₂O₄) as also mentioned in earlier studies (Brand et al., 1998; Proenza et al., 2008). Willemseite [(Ni,Mg)₃Si₄O₁₀(OH)₂] and other garnierite minerals may be also sources of Ni in saprolitic ores (Tauler et al., 2009; Villanova-De-Benavent et al., 2017; Zhu et al., 2012). Hematite (Fe₂O₃) and Talc [Mg₃Si₂O₁₀(OH)₂] are also present in the ore as minor mineral phases.

The XRD patterns of the leaching residues, obtained after leaching with H₂SO₄ solution containing Na₂SO₃, are shown in Fig. 5(b, c). It is shown that the characteristic peaks of lizardite/nepouite at 2-theta = 12.108 which were present in the initial ore were not present in the leaching residues, indicating that most of these minerals were leached, at least to a degree that does not allow their identification through XRD. On the other hand, the intensities of characteristic peaks of quartz and goethite/hematite increased in the XRD patterns of the residues obtained after H₂SO₄ leaching, especially in the presence of Na₂SO₃. H₂SO₄ leaching without or with the addition of Na₂SO₃ resulted in the formation in the LKr of bassanite (CaSO₄·0.5H₂O) or gypsum (CaSO₄·2H₂O) respectively, due to the relatively high CaO content (7.16%) in the LK ore.

The FTIR spectra of LK and LKr are shown in Fig. 6. In all samples, bending and stretching vibrational bands of Si—O—Si and O—Si—O can be observed at 450–460 cm⁻¹ and ~800 cm⁻¹, respectively (Andini et al., 2008). The next peaks, seen only in LKr, between 600 and 667 cm⁻¹ are due to the formation of calcium-based sulfates. These results are consistent with the data derived from the corresponding XRD patterns (Fig. 5). Moreover, the characteristic asymmetric stretching vibration of Si—O—T (T=Al or Si) in the LK at 1014 cm⁻¹ is shifted toward higher wavenumbers (1092 and 1150 cm⁻¹) in LKr. This upward shift indicates that Si—O bonds dominate LKr due to the destruction/decomposition of the initial Mg-Al-silicate matrix (Baščarević et al., 2013) and the subsequent formation and precipitation of Ca-sulfates. Two small shoulders at 876 cm⁻¹ and 2512 cm⁻¹ seen in the LK ore along with a weak band at 1422 cm⁻¹ can be attributed to stretching vibrations of O—C—O bonds indicating the presence of calcite, as shown in XRD patterns. The decrease of the intensity of the stretching vibration of the inner —OH group at ~3680 cm⁻¹ means that most nickel has been extracted from the LK ore (Scholtzová et al., 2003).

Fig. 7 shows the DSC/TG curves for LK and its residues during heating. The low-temperature endothermic peaks seen at 110 °C and 140 °C (Fig. 7(a–c)) are associated with the loss of free water. The endothermic peaks seen between 300 and 315 °C in all samples are attributed to the dehydroxylation of goethite (FeOOH) to form hematite (α-Fe₂O₃) or the decomposition of other hydroxyls (Elfad et al., 2018). The endothermic peak at 640 °C for LK (Fig. 7a) shows the

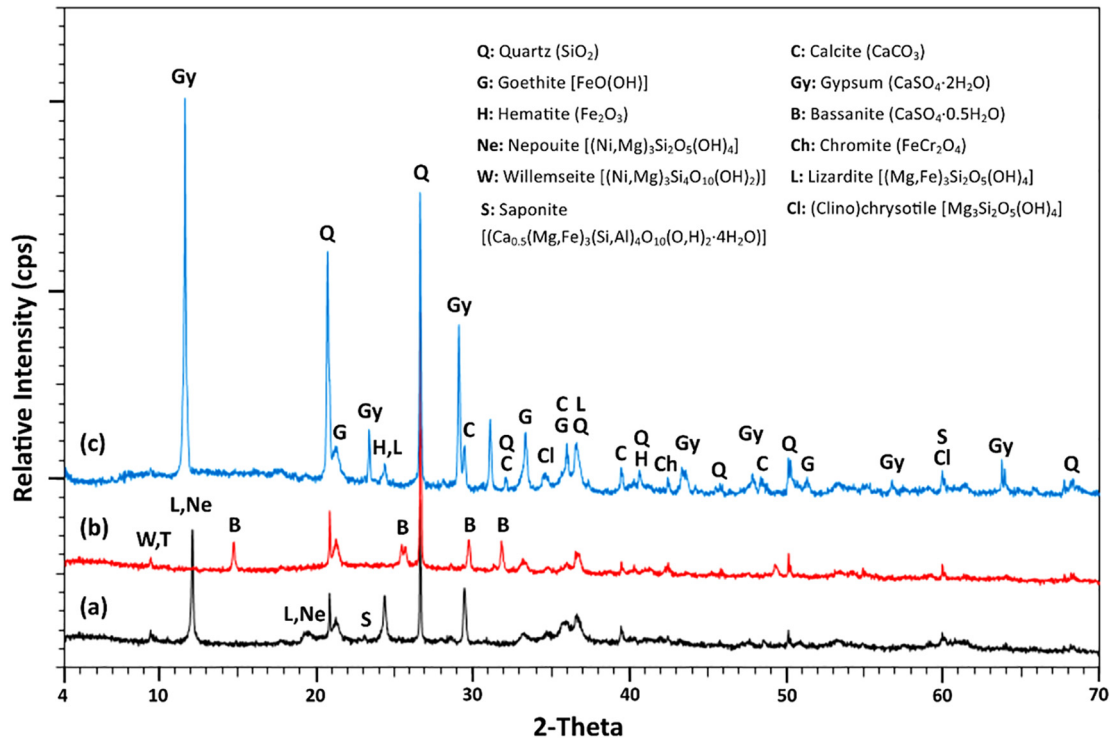


Fig. 5. XRD patterns of (a) LK ore, (b) LKr obtained after leaching with 147 g L⁻¹ H₂SO₄ solution and (c) LKr obtained after leaching with 147 g L⁻¹ H₂SO₄ solution containing 20 g L⁻¹ Na₂SO₃.

decomposition of nickeliferous lizardite which loses its crystal water and transforms to olivine (Febriana et al., 2018; Mu et al., 2018); this peak is not shown in LKr since most lizardite has been leached. The peaks at 590 °C and 840 °C shown in the residues are due to recrystallization of magnesium silicates to forsterite (Mg₂SiO₄) (Tartaj et al., 2000; Zevgolis et al., 2010).

BSE images of the LK ore and LKr obtained after leaching with H₂SO₄ solution without and with the addition of Na₂SO₃ are shown in Fig. 8(a–d).

SEM analysis of the LK ore along with EDS point analyses (Fig. 8(a, b)) revealed that nepouite, chromite and vitreous goethite were the main Ni-bearing mineral phases, containing up to 3.16%, 5.89% and 0.95% Ni, respectively. As shown in XRD patterns, the major mineralogical phases, namely quartz, calcite, and hematite were also detected in the LK ore; other silicates such as talc and clinochrysotile were also detected in some places. Fig. 8(b) (zoom of rectangular area of Fig. 8(a)) shows in detail the presence of nepouite and lizardite along cracks

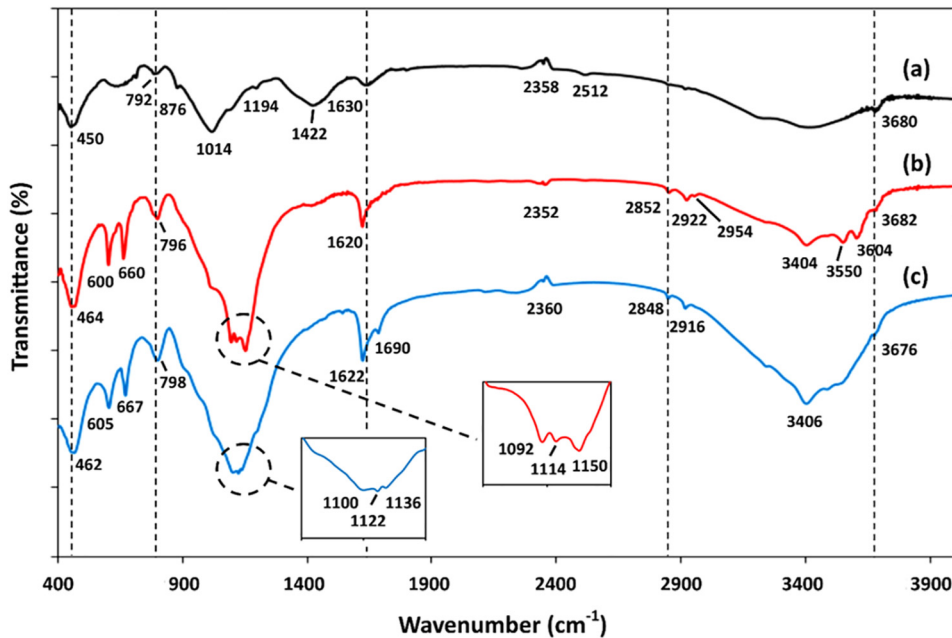


Fig. 6. FTIR spectra of (a) LK ore, (b) LKr obtained after leaching with 147 g L⁻¹ H₂SO₄ solution, and (c) LKr obtained after leaching with 147 g L⁻¹ H₂SO₄ solution containing 20 g L⁻¹ Na₂SO₃.

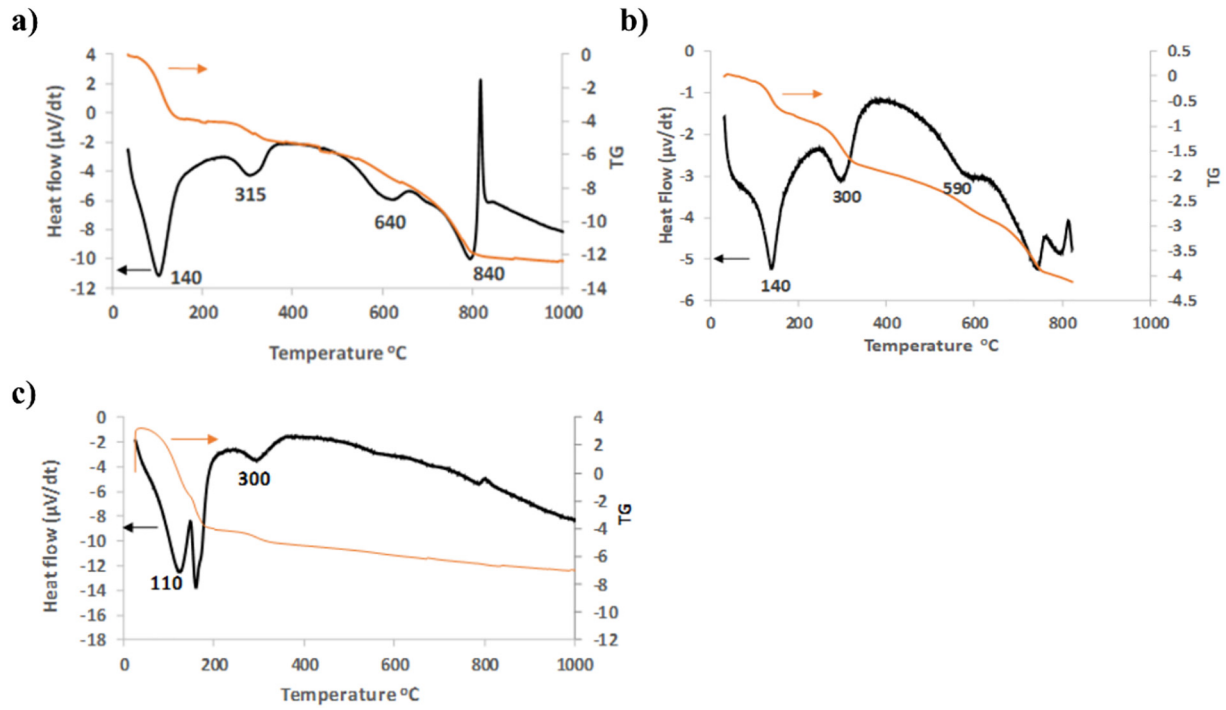


Fig. 7. DSC/TG curves of (a) LK, (b) LKr obtained after leaching with $147 \text{ g L}^{-1} \text{ H}_2\text{SO}_4$ solution, and (c) LKr obtained after leaching with $147 \text{ g L}^{-1} \text{ H}_2\text{SO}_4$ solution containing $20 \text{ g L}^{-1} \text{ Na}_2\text{SO}_3$.

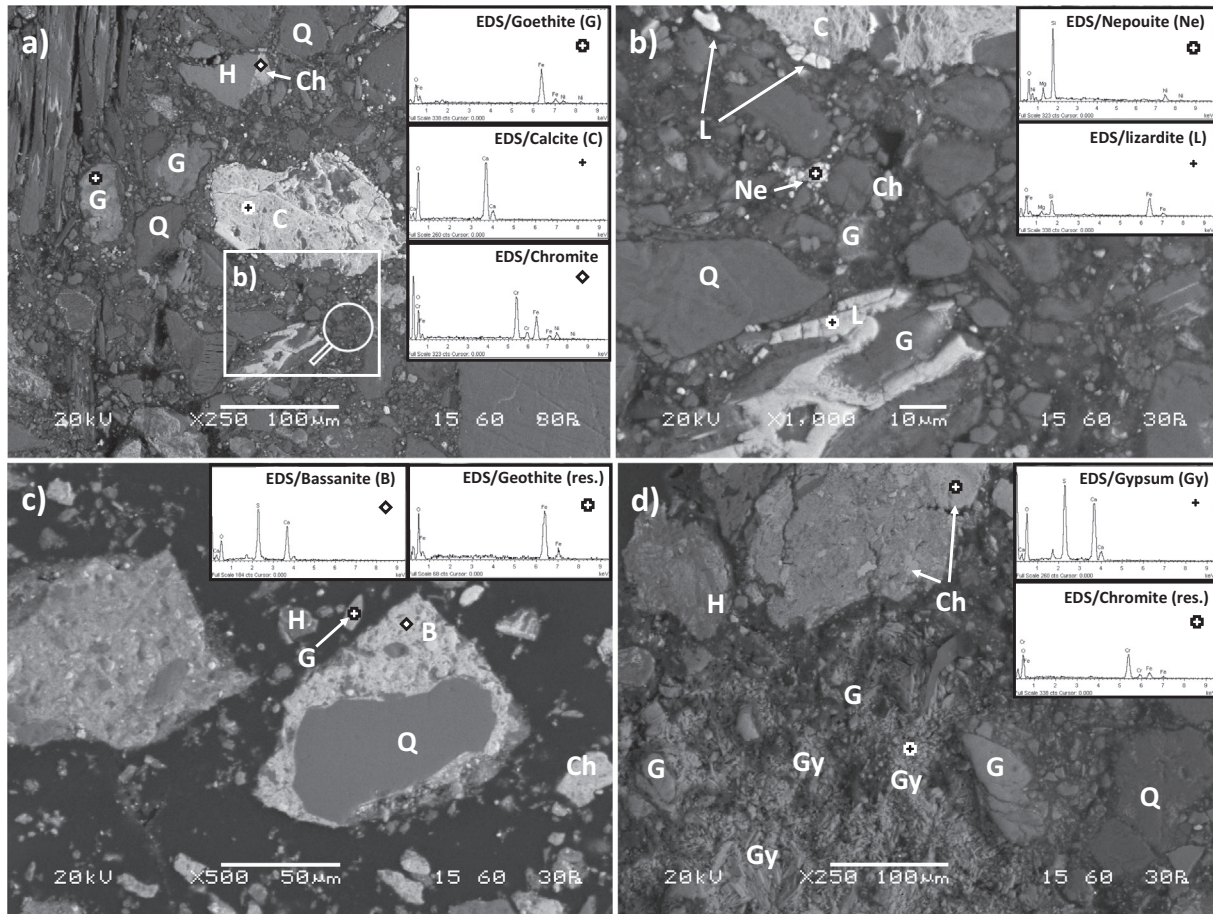


Fig. 8. Back-scattered electron images of the LK ore (a and b) and LKr obtained after leaching with c) H_2SO_4 and d) H_2SO_4 with the addition of Na_2SO_3 . EDS spectra show in several spot locations the presence of Ni-bearing mineral phases and the formation of mixed aggregates and newly formed phases after leaching (Q: Quartz, C: Calcite, G: Geothite, H: Hematite, Ne: Nepouite, Ch: Chromite, L: Lizardite, B: Bassanite, Gy: Gypsum).

and grain boundaries. As can be seen in Fig. 8(b), nepouite (Ni-rich analogue of lizardite) is observed as flaky-like infillings present at the boundaries between goethite and quartz, while long tabular lizardite crystals were found along shrinkage cracks at the internal space of goethite (Zhu et al., 2012) or at the boundaries of calcite. Furthermore, chromite crystals were usually severely cracked and the cracks were filled with Ni-rich goethite.

After LK leaching with H₂SO₄ without or with the addition of Na₂SO₃ (Fig. 8(c, d)), LKr displayed quite smooth edges and surfaces which mostly comprised of newly formed aggregates formed by a large number of small particles of the LK ore that agglomerated (Çetintaş et al., 2018). It is seen that Ni-rich nepouite and calcite were not observed in LKr obtained after leaching, thus indicating that they were both depleted after reacting with the leaching medium, while the more refractory particles of hematite, goethite and quartz reacted only partially.

It is important to note that bassanite formed an outer shell of fine crystals often mixed with silicate aggregates adjacent to quartz or iron (oxy)hydroxides surfaces, while gypsum almost dominated the whole interlocking crystalline matrix of the solid residues. Finally, SEM micrographs and EDS analyses of LKr also revealed a porous structure for the goethite and chromite particles as a result of the acid attack, which resulted in partial or even complete leaching of the contained nickel (Fig. 8(c, d)). The presence of these Ni-free phases and the absence of nepouite indicate that most Ni was extracted from the LK ore during leaching.

3.5. Assessment of toxicity

Table 7 presents the toxicity of LKr as well as of the IPs produced after alkali activation of the leaching residues, as derived from the application of the EN 12457-3 test.

Regarding LKr it is seen that the toxicity limits are exceeded by far only for Ni, when both distilled water (pH 7.0) or HCl (pH 4.0) are used as leaching solutions. In the second case, the degree of dissolution rate of Ni is almost doubled to 447 mg kg⁻¹. After alkali activation the dissolution rate of Ni from the IPs decreases dramatically to values well below the limits, 1.13 mg kg⁻¹. This indicates the potential of alkali activation not only to result in the production of materials with beneficial properties but also to bind or trap potentially hazardous elements in a stable matrix and therefore reduce their solubilization potential (Komnitsas et al., 2013). The results also show that the dissolution of all other elements from the IPs is well below the lowest limits when

the leaching solution is water, thus the specimens present no toxicity according to the EN 12457-3 test. When the leaching solution becomes more aggressive (HCl solution, pH 4) the dissolution of Ni, As and Pb exceeds slightly the lowest limits, thus suggesting that the structural integrity of the produced specimens is very good.

4. Conclusions

This study confirms the potential of column leaching of a low-grade Greek saprolitic laterite for the extraction of Ni and Co. Experimental results indicate that within a very short period, 72.5% of Ni and 47.4% of Co can be extracted from the ore, when leaching is carried out using a solution containing 147 g L⁻¹ H₂SO₄ and 20 g L⁻¹ Na₂SO₃. Furthermore, it is mentioned that the obtained Fe and Al co-extractions are low, 8.7% and 31.3% respectively, thus indicating that the process is characterized by good selectivity, as also confirmed by the ratios Ni/Fe and Ni/Al in the PLS.

In addition, the beneficial effect of the presence of H₂SO₃ in the leaching medium is due to the fact that the generated SO₂ reacts with iron-based phases, accelerates their dissolution and subsequently results in the extraction of the contained Ni.

Leaching residues can be alkali activated with the use of NaOH and Na₂SiO₃ as activators and the addition of 10 wt% metakaolin so that IPs with high strength, almost 40 MPa, can be produced. These products have very low toxicity and can be used as binders or building materials in several applications in the construction sector.

The approach followed in this study is environment friendly since it treats low grade nickel ores for the production of critical metals such as Ni and Co and thus contributes to raw materials savings, while it valorizes successfully the leaching residues and produces IPs with high added value.

Acknowledgements

The authors would like to acknowledge the financial support of European Commission in the frame of Horizon 2020 project “Metal recovery from low-grade ores and wastes”, www.metgrowplus.eu, Grant Agreement no. 690088. The assistance of Mrs. Olga Pantelaki and Dr. Anna Kritikaki in carrying out tests and analyses is also acknowledged. Finally, the authors acknowledge the contribution of the three anonymous reviewers in improving the quality of the manuscript.

Table 7

Toxicity of LKr and IPs according to the EN 12457-3 (L/S = 10 L kg⁻¹) compliance test.

| Element | LKr (mg kg ⁻¹) ^a | | IP (mg kg ⁻¹) ^a | | Toxicity limits (mg kg ⁻¹) ^b | | | |
|--------------------|---|------------|--|------------|--|------------------------|---|---|
| | H ₂ O (pH 7) | HCl (pH 4) | H ₂ O (pH 7) | HCl (pH 4) | For waste accepted at landfills for inert waste ^c | For nonhazardous waste | For hazardous waste accepted at landfills for non-hazardous waste | For waste accepted at landfills for hazardous waste |
| Fe | 11.53 | 52.72 | 9.69 | 0.04 | | | | |
| Mn | 24.16 | 41.16 | 0.18 | 0.50 | | | | |
| Al | 30.00 | 82.64 | 165.16 | 382.46 | | | | |
| Ni | 256.53 | 447.11 | 0.31 | 1.13 | 0.4 | 10 | 10 | 40 |
| Cu | 1.89 | 0.31 | 0.43 | 0.69 | 2 | 50 | 50 | 100 |
| Zn | 1.89 | 1.10 | 0.67 | 2.51 | 4 | 50 | 50 | 200 |
| As | 0.01 | 0.02 | 0.12 | 1.47 | 0.5 | 2 | 2 | 25 |
| Mo | 0.01 | 0.32 | 0.22 | 0.17 | 0.5 | 10 | 10 | 30 |
| Cd | <DL | <DL | <DL | <DL | 0.04 | 1 | 1 | 5 |
| C _{Total} | 0.24 | 1.07 | 0.38 | 1.75 | 0.5 | 10 | 10 | 50 |
| Pb | <DL | <DL | 0.15 | 3.18 | 0.5 | 10 | 10 | 50 |

^aDL: detection limit.

^bCouncil Decision 19 Dec. 2002 (2003/33/EC).

^cShaded parts indicate elements that exceed limits.

References

- Agatzini-Leonardou, S., Dimaki, D., 1994. Heap leaching of poor nickel laterites by sulphuric acid at ambient temperature. *Hydrometallurgy* 94. 1994. Springer, Dordrecht, The Netherlands, pp. 193–208. https://doi.org/10.1007/978-94-011-1214-7_11.
- Agatzini-Leonardou, S., Zafiratos, I.G., 2004. Beneficiation of a Greek serpentinic nickeliferous ore part II. Sulphuric acid heap and agitation leaching. *Hydrometallurgy* 74, 267–275. <https://doi.org/10.1016/j.hydromet.2004.05.006>.
- Agatzini-Leonardou, S., Zafiratos, J.G., Spathis, D., 2004. Beneficiation of a Greek serpentinic nickeliferous ore: part I. Mineral processing. *Hydrometallurgy* 74, 259–265. <https://doi.org/10.1016/j.hydromet.2004.05.005>.
- Agatzini-Leonardou, S., Tsakiridis, P.E., Oustadakis, P., Karidakis, T., Katsiapi, A., 2009. Hydrometallurgical process for the separation and recovery of nickel from sulphate heap leach liquor of nickeliferous laterite ores. *Miner. Eng.* 22, 1181–1192. <https://doi.org/10.1016/j.mineng.2009.06.006>.
- Andini, S., Cioffi, R., Colangelo, F., Grieco, T., Montagnaro, F., Santoro, L., 2008. Coal fly ash as raw material for the manufacture of geopolymer-based products. *Waste Manag.* 28, 416–423. <https://doi.org/10.1016/j.wasman.2007.02.001>.
- Bartzas, G., Komnitsas, K., 2015. Life cycle assessment of ferronickel production in Greece. *Resour. Conserv. Recycl.* 105, 113–122. <https://doi.org/10.1016/j.resconrec.2015.10.016>.
- Bašćarević, Z., Komljenović, M., Miladinović, Z., Nikolić, V., Marjanović, N., Žujović, Z., Petrović, R., 2013. Effects of the concentrated NH_4NO_3 solution on mechanical properties and structure of the fly ash based geopolymers. *Constr. Build. Mater.* 41, 570–579. <https://doi.org/10.1016/j.conbuildmat.2012.12.067>.
- Brand, N.W., Butt, C.R.M., Elias, M., 1998. Nickel laterites: classification and features. *J. Aust. Geol. Geophys.* 17 (4), 81–88.
- Büyükkıncı, E., 2008. Extraction of Nickel From Lateritic Ores. (Master of Science Thesis). Middle East Technical University, Turkey <https://etd.lib.metu.edu.tr/upload/12609291/index.pdf>, Accessed date: 10 November 2018.
- Canterford, J.H., 1986. Acid leaching of chromite-bearing nickeliferous laterite from Rockhampton, Queensland. *AusIMM Bull.* 291 (6), 51–56.
- Çetintaş, S., Yıldız, U., Bingöl, D., 2018. A novel reagent-assisted mechanochemical method for nickel recovery from lateritic ore. *J. Clean. Prod.* 199, 616–632. <https://doi.org/10.1016/j.jclepro.2018.07.212>.
- Chaerun, S.K., Sulistyo, R.S., Minwal, W.P., Mubarak, M.Z., 2017. Indirect bioleaching of low-grade nickel limonite and saprolite ores using fungal metabolic organic acids generated by *Aspergillus Niger*. *Hydrometallurgy* 174, 29–37. <https://doi.org/10.1016/j.hydromet.2017.08.006>.
- Das, G.K., de Lange, J.A.B., 2011. Reductive atmospheric acid leaching of West Australian smectitic nickel laterite in the presence of sulphur dioxide and copper(II). *Hydrometallurgy* 105, 264–269. <https://doi.org/10.1016/j.hydromet.2010.10.016>.
- du Plessis, C.A., Slabbert, W., Hallberg, K.B., Johnson, D.B., 2011. Ferredox: a biohydrometallurgical processing concept for limonitic nickel laterites. *Hydrometallurgy* 109 (3–4), 221–229. <https://doi.org/10.1016/j.hydromet.2011.07.005>.
- Eckelman, M.J., 2010. Facility-level energy and greenhouse gas life-cycle assessment of the global nickel industry. *Resour. Conserv. Recycl.* 54, 256–266. <https://doi.org/10.1016/j.resconrec.2009.08.008>.
- Elfiad, A., Galli, F., Djadoun, A., Sennour, M., Chegrouche, S., Meddour-Boukhobza, L., Boffito, D.C., 2018. Natural $\alpha\text{-Fe}_2\text{O}_3$ as an efficient catalyst for the p-nitrophenol reduction. *Mater. Sci. Eng. B* 229, 126–134. <https://doi.org/10.1016/j.mseb.2017.12.009>.
- Elliot, A., Fletcher, H., Li, J., Watling, H., Robinson, D.J., 2009. Heap leaching of nickel laterites—a challenge and an opportunity. In: Budac, J.J., Fraser, R., Mihaylov, I., Papangelakis, V.G., Robinson, D.J. (Eds.), *Hydrometallurgy of Nickel and Cobalt 2009*, Proceedings of the 39th Annual Hydrometallurgy Meeting Held in the Conjunction With the 48th Annual Conference of Metallurgists; Sudbury, Canada, 23–26 August. 2009. Canadian Institute of Mining, Metallurgy and Petroleum, Montreal, pp. 537–549.
- EN12457-3, 2002. Characterization of Waste – Compliance Test for Leaching of Granular Waste Materials and Sludges – Part 3: Two Stage Batch Test at a Liquid to Solid Ratio of 2 l/kg and 8 l/kg for Materials With High Solid Content and With Particle Size Below 4 mm. 2002. European Committee for Standardization, Brussels.
- EU Science Hub, 2019. The European Commission's science and knowledge service. <https://ec.europa.eu/jrc/en/news/cobalt-potential-bottleneck-transition-electricmobility>, Accessed date: 14 January 2019.
- European Commission, 2002. Council Decision of 19 December 2002 establishing criteria and procedures for the acceptance of waste at landfills pursuant to Article 16 of and Annex II to Directive 1999/31/EC. <https://eur-lex.europa.eu/legal-content/EN/TXT/PDF/?uri=CELEX:32003D0033&from=EN>, Accessed date: 10 November 2018.
- Febriana, E., Manaf, A., Prasetyo, A.B., Mayangsari, W., 2018. Thermal characteristic of limonite ore upon calcination and reduction. Proceedings of the International Seminar on Metallurgy and Materials (ISMM2017), AIP Conference Proceedings. vol. 1964, p. 020026. <https://doi.org/10.1063/1.5038308>.
- Georgiou, D., Papangelakis, V., 1998. Sulphuric acid pressure leaching of a limonitic laterite: chemistry and kinetics. *Hydrometallurgy* 49, 23–46. [https://doi.org/10.1016/S0304-386X\(98\)00023-1](https://doi.org/10.1016/S0304-386X(98)00023-1).
- Guo, Q., Qu, J., Han, B., Zhang, P., Song, Y., Qi, T., 2015. Innovative technology for processing saprolitic laterite ores by hydrochloric acid atmospheric pressure leaching. *Miner. Eng.* 71, 1–6. <https://doi.org/10.1016/j.mineng.2014.08.010>.
- Hunter, H.M.A., Herrington, R.J., Oxley, E.A., 2013. Examining Ni-laterite leach mineralogy & chemistry – a holistic multi-scale approach. *Miner. Eng.* 54, 100–119. <https://doi.org/10.1016/j.mineng.2013.05.002>.
- Jang, H.-C., Marjorie Valix, M., 2017. Overcoming the bacteriostatic effects of heavy metals on *Acidithiobacillus thiooxidans* for direct bioleaching of saprolitic Ni laterite ores. *Hydrometallurgy* 168, 21–25. <https://doi.org/10.1016/j.hydromet.2016.08.016>.
- Khoo, J.Z., Haque, N., Woodbridge, G., McDonald, R., Bhattacharya, S., 2017. A life cycle assessment of a new laterite processing technology. *J. Clean. Prod.* 142 (4), 1765–1777. <https://doi.org/10.1016/j.jclepro.2016.11.111>.
- Komnitsas, K., 1983. Kinetic Study of Laterite Leaching With Sulphuric Acid at Atmospheric Pressure. (Diploma thesis). National Technical University of Athens (in Greek).
- Komnitsas, K., 1988. High Pressure Acid Leaching of Laterites. (PhD thesis). National Technical University of Athens (in Greek, English abstract). <https://www.didaktorika.gr/eadd/handle/10442/1521?locale=en>, Accessed date: 9 November 2018.
- Komnitsas, K., Zaharaki, D., 2007. Geopolymerisation. A review and prospects for the minerals industry. *Miner. Eng.* 20, 1261–1277. <https://doi.org/10.1016/j.mineng.2007.07.011>.
- Komnitsas, K., Zaharaki, D., Perdikatsis, V., 2007. Geopolymerisation of low calcium ferronickel slags. *J. Mater. Sci.* 42 (9), 3073–3082. <https://doi.org/10.1007/s10853-006-0529-2>.
- Komnitsas, K., Zaharaki, D., Perdikatsis, V., 2009. Effect of synthesis parameters on the compressive strength of low-calcium ferronickel slag inorganic polymers. *J. Hazard. Mater.* 161, 760–768. <https://doi.org/10.1016/j.jhazmat.2008.04.055>.
- Komnitsas, K., Zaharaki, D., Bartzas, G., 2013. Effect of sulphate and nitrate anions on heavy metal immobilisation in ferronickel slag geopolymers. *Appl. Clay Sci.* 73, 103–109. <https://doi.org/10.1016/j.clay.2012.09.018>.
- Komnitsas, K., Petrakis, E., Pantelaki, O., Kritikaki, A., 2018. Column leaching of greek low-grade limonitic laterites. *Minerals* 8 (9), 377. <https://doi.org/10.3390/min8090377>.
- Kontopoulos, A., Komnitsas, K., 1988. Sulphuric acid pressure leaching of low-grade Greek laterites. In: Yulian, Zheng, Jiazhong, Xu (Eds.), *Proceedings of the 1st International Symposium on Hydrometallurgy*. 1988. Pergamon Press, Oxford, United Kingdom, pp. 140–144 (Beijing, China, 12–15 October).
- Kwon, Y.H., Kang, S.H., Hong, A.G., Moon, J., 2017. Intensified pozzolanic reaction on kaolinite clay-based mortar. *Appl. Sci.* 7, 522. <https://doi.org/10.3390/app7050522>.
- Le, L., Tang, J., Ryan, D., Valix, M., 2006. Bioleaching nickel laterite ores using multi-metal tolerant *Aspergillus foetidus* organism. *Miner. Eng.* 19, 1259–1265. <https://doi.org/10.1016/j.mineng.2006.02.006>.
- Li, J., Li, X., Hu, Q., Wang, Z., Zhou, Y., Zheng, J., Liu, W., Li, L., 2009. Effect of pre-roasting on leaching of laterite. *Hydrometallurgy* 99, 84–88. <https://doi.org/10.1016/j.hydromet.2009.07.006>.
- Li, G., Zhou, Q., Zhu, Z., Luo, J., Rao, M., Peng, Z., Jiang, T., 2018a. Selective leaching of nickel and cobalt from limonitic laterite using phosphoric acid: an alternative for value-added processing of laterite. *J. Clean. Prod.* 189, 620–626. <https://doi.org/10.1016/j.jclepro.2018.04.083>.
- Li, J., Li, D., Xu, Z., Liao, C., Liu, Y., Zhong, B., 2018b. Selective leaching of valuable metals from laterite nickel ore with ammonium chloride - hydrochloric acid solution. *J. Clean. Prod.* 179, 24–30. <https://doi.org/10.1016/j.jclepro.2018.01.085>.
- Liu, K., Chen, Q., Yin, Z., Hu, H., Ding, Z., 2012. Kinetics of leaching of a Chinese laterite containing magnetite and magnetite in sulfuric acid solutions. *Hydrometallurgy* 125–126, 125–136. <https://doi.org/10.1016/j.hydromet.2012.06.001>.
- Loveday, B.K., 2008. The use of oxygen in high pressure acid leaching of nickel laterites. *Miner. Eng.* 21, 533–538. <https://doi.org/10.1016/j.mineng.2007.11.002>.
- Luo, W., Feng, Q., Ou, L., Zhang, G., Lu, Y., 2009. Fast dissolution of nickel from a lizardite rich saprolitic laterite by sulphuric acid at atmospheric pressure. *Hydrometallurgy* 96 (1–2), 171–175. <https://doi.org/10.1016/j.hydromet.2008.08.001>.
- Luo, W., Feng, Q., Ou, L., Zhang, G., Chen, Y., 2010. Kinetics of saprolitic laterite leaching by sulphuric acid at atmospheric pressure. *Miner. Eng.* 23, 458–462. <https://doi.org/10.1016/j.mineng.2009.10.006>.
- Luo, J., Li, G., Rao, M., Peng, Z., Zhang, Y., Jiang, T., 2015. Atmospheric leaching characteristics of nickel and iron in limonitic laterite with sulfuric acid in the presence of sodium sulfite. *Miner. Eng.* 78, 38–44. <https://doi.org/10.1016/j.mineng.2015.03.030>.
- Ma, B., Yang, W., Yang, B., Wang, C., Chen, Y., Zhang, Y., 2015. Pilot-scale plant study on the innovative nitric acid pressure leaching technology for laterite ores. *Hydrometallurgy* 155, 88–94. <https://doi.org/10.1016/j.hydromet.2015.04.016>.
- MacCarthy, J., Nosrati, A., Skinner, W., Addai-Mensah, J., 2015. Acid leaching and rheological behaviour of a siliceous goethitic nickel laterite ore: influence of particle size and temperature. *Miner. Eng.* 77, 52–63. <https://doi.org/10.1016/j.mineng.2014.12.031>.
- MacCarthy, J., Nosrati, A., Skinner, W., Addai-Mensah, J., 2016. Atmospheric acid leaching mechanisms and kinetics and rheological studies of a low grade saprolitic nickel laterite ore. *Hydrometallurgy* 160, 26–37. <https://doi.org/10.1016/j.hydromet.2015.11.004>.
- McDonald, R.G., Whittington, B.J., 2008. Atmospheric acid leaching of nickel laterites review: part I. Sulphuric acid technologies. *Hydrometallurgy* 91, 35–55. <https://doi.org/10.1016/j.hydromet.2007.11.009>.
- Mu, W., Lu, X., Cui, F., Luo, S., Zhai, Y., 2018. Transformation and leaching kinetics of silicon from low-grade nickel laterite ore by pre-roasting and alkaline leaching process. *Trans. Nonferrous Metals Soc. China* 28 (1), 169–176. [https://doi.org/10.1016/S1003-6326\(18\)64650-3](https://doi.org/10.1016/S1003-6326(18)64650-3).
- Myagkiy, A., Truche, L., Cathelineau, M., Golfier, F., 2017. Revealing the conditions of Ni mineralization in the laterite profiles of New Caledonia: insights from reactive geochemical transport modeling. *Chem. Geol.* 466, 274–284. <https://doi.org/10.1016/j.chemgeo.2017.06.018>.
- Mystrioti, C., Passiopi, N., Xenidis, A., Komnitsas, K., 2018. Comparative evaluation of sulfuric and hydrochloric acid atmospheric leaching for the treatment of Greek low grade nickel laterites. In: Davis, B., et al. (Eds.), *Extraction 2018. The Minerals, Metals & Materials Series*. Springer, Cham, pp. 1753–1764 https://doi.org/10.1007/978-3-319-95022-8_145.
- Nickel Institute, 2019. Nickel mining & production. <https://www.nickelinstitute.org/about-nickel/>, Accessed date: 14 January 2019.
- Norgate, T., Jahanshahi, S., 2011. Assessing the energy and greenhouse gas footprints of nickel laterite processing. *Miner. Eng.* 24 (7), 698–707. <https://doi.org/10.1016/j.mineng.2010.10.002>.

- Nosrati, A., Quast, K., Xu, D., Skinner, W., Robinson, D.J., Addai-Mensah, J., 2014. Agglomeration and column leaching behaviour of nickel laterite ores: effect of ore mineralogy and particle size distribution. *Hydrometallurgy* 146, 29–39. <https://doi.org/10.1016/j.hydromet.2014.03.004>.
- Oxley, A., Smith, M.E., Caceres, O., 2016. Why heap leach nickel laterites? *Miner. Eng.* 88, 53–60. <https://doi.org/10.1016/j.mineng.2015.09.018>.
- Panagiotopoulos, N., Agatzini, S., Kontopoulos, A., 1986. Extraction of Nickel and Cobalt From Serpentinic Type Laterites by Atmospheric Pressure Sulfuric Acid Leaching, 115th TMS-AIME Annual Meeting, New Orleans, Paper no A86–30.
- Petrakis, E., Karmali, V., Komnitsas, K., 2018. Factors affecting nickel upgrade during selective grinding of low-grade limonitic laterites. *Miner. Process. Ext. Metall.*, 1–10 <https://doi.org/10.1080/25726641.2018.1521578>.
- Pickles, C.A., Anthony, W., 2018. Thermodynamic modelling of the reduction of a saprolitic laterite ore by methane. *Miner. Eng.* 120, 47–59. <https://doi.org/10.1016/j.mineng.2018.02.006>.
- Proenza, J.A., Lewis, J.F., Galí, S., Tauler, E., Labrador, M., Melgarejo, J.C., Longo, F., Bloise, G., 2008. Garnierite Mineralization From Falcondo Ni-Laterite Deposit (Dominican Republic). 9. *Macla*, pp. 197–198. <http://diposit.ub.edu/dspace/bitstream/2445/107902/1/562923.pdf>, Accessed date: 13 November 2018.
- Quaicoe, I., Nosrati, A., Skinner, W., Addai-Mensah, J., 2014. Agglomeration and column leaching behaviour of goethitic and saprolitic nickel laterite ores. *Miner. Eng.* 65, 1–8. <https://doi.org/10.1016/j.mineng.2014.04.001>.
- Quast, K., Xu, D., Skinner, W., Nosrati, A., Hilder, T., Robinson, D.J., Addai-Mensah, J., 2013. Column leaching of nickel laterite agglomerates: effect of feed size. *Hydrometallurgy* 134–135, 144–149. <https://doi.org/10.1016/j.hydromet.2013.02.001>.
- Quast, K., Connor, J.N., Skinner, W., Robinson, D.J., Addai-Mensah, J., 2015. Preconcentration strategies in the processing of nickel laterite ores part 1: literature review. *Miner. Eng.* 79, 261–268. <https://doi.org/10.1016/j.mineng.2015.03.017>.
- Rubisov, D.H., Papangelakis, V.G., 2000. Sulphuric acid pressure leaching of laterites - a comprehensive model of a continuous autoclave. *Hydrometallurgy* 58 (2), 89–101. [https://doi.org/10.1016/S0304-386X\(00\)00092-X](https://doi.org/10.1016/S0304-386X(00)00092-X).
- Scholtzová, E., Tunega, D., Turi Nagy, L., 2003. Theoretical study of cation substitution in trioctahedral sheet of phyllosilicates. An effect on inner OH group. *J. Mol. Struct. (THEOCHEM)* 620 (1), 1–8. [https://doi.org/10.1016/S0166-1280\(02\)00320-2](https://doi.org/10.1016/S0166-1280(02)00320-2).
- Sullivan, M.S., Chorzepa, M.G., Hamid, H., Durham, S.A., Kim, S.S., 2018. Sustainable materials for transportation infrastructures: comparison of three commercially metakaolin products in binary, cementitious systems. *Infrastructures* 3 (3), 17. <https://doi.org/10.3390/infrastructures3030017>.
- Tartaj, P., Cerpa, A., Garcia-Gonzalez, M.T., Serna, C.J., 2000. Surface instability of serpentine in aqueous suspensions. *J. Colloid Interface Sci.* 231 (1), 176–181. <https://doi.org/10.1006/jcis.2000.7109>.
- Tauler, E., Proenza, J., Galí, S., Lewis, J., Labrador, M., García-Romero, E., 2009. Ni-sepiolite-falcondoite in garnierite mineralisation from the Falcondo Ni-laterite deposit, Dominican Republic. *Clay Miner.* 44 (4), 435–454. <https://doi.org/10.1180/claymin.2009.044.4.435>.
- Thubakgale, C.K., Mbaya, R.K.K., Kabongo, K., 2013. A study of atmospheric acid leaching of a South African nickel laterite. *Miner. Eng.* 54, 79–81. <https://doi.org/10.1016/j.mineng.2013.04.006>.
- van der Sloot, H.A., Hjelmar, O., Bjerre Hansen, J., Woiitke, P., Lepom, P., Leschber, R., Bartet, B., Debrucker, N., 2001. Validation of CEN/TC 292 Leaching Tests and Eluate Analysis Methods prEN 12457 1–4, ENV 13370 and ENV 12506.
- Villanova-De-Benavent, C., Domènech, C., Tauler, E., Galí, S., Tassara, S., Proenza, J., 2017. Fe–Ni-bearing serpentines from the saprolite horizon of Caribbean Ni-laterite deposits: new insights from thermodynamic calculations. *Mineral. Deposita* 52 (7), 979–992. <https://doi.org/10.1007/s00126-016-0683-7>.
- Watling, H.R., Elliot, A.D., Fletcher, H.M., Robinson, D.J., Sully, D.M., 2011. Ore mineralogy of nickel laterites: controls on processing characteristics under simulated heap-leach conditions. *Aust. J. Earth Sci.* 58 (7), 725–744. <https://doi.org/10.1080/08120099.2011.602986>.
- Zaharaki, D., Galetakis, M., Komnitsas, K., 2016. Valorization of construction and demolition (C&D) and industrial wastes through alkali activation. *Constr. Build. Mater.* 121, 686–693. <https://doi.org/10.1016/j.conbuildmat.2016.06.051>.
- Zanbak, C., 2012. Heap leaching technique in mining within the context of best available techniques (BAT), November 2012. <http://www.euromines.org/files/mining-europe/mining-techniques/batforheappleaching-feb2013-c.zanbak-euromines.pdf>, Accessed date: 7 November 2018.
- Zevgolis, E., Zografidis, C., Halikia, I., 2010. The reducibility of the Greek nickeliferous laterites: a review. *Miner. Process. Ext. Metall.* 119 (1), 9–17. <https://doi.org/10.1179/174328509x431472>.
- Zhang, P., Guo, Q., Wei, G., Meng, L., Han, L., Qu, J., Qi, T., 2015. Extraction of metals from saprolitic laterite ore through pressure hydrochloric-acid selective leaching. *Hydrometallurgy* 157, 149–158. <https://doi.org/10.1016/j.hydromet.2015.08.007>.
- Zhang, P., Guo, Q., Wei, G., Meng, L., Han, L., Qu, J., Qi, T., 2016. Leaching metals from saprolitic laterite ore using a ferric chloride solution. *J. Clean. Prod.* 112, 3531–3539. <https://doi.org/10.1016/j.jclepro.2015.10.134>.
- Zhu, D.-Q., Cui, Y., Hapugoda, S., Vining, K., Pan, J., 2012. Mineralogy and crystal chemistry of a low grade nickel laterite ore. *Trans. Nonferrous Metals Soc. China* 22 (4), 907–916. [https://doi.org/10.1016/S1003-6326\(11\)61264-8](https://doi.org/10.1016/S1003-6326(11)61264-8).